Bioconjugate Chemistry

Article

pubs.acs.org/bc

In Vivo Self-Assembly of Fluorescent Protein Microparticles Displaying Specific Binding Domains

Anika C. Jahns,[†] Yogananda Maspolim,[†] Shuxiong Chen,[†] Jenness M. Guthrie,[†] Len F. Blackwell,[†] and Bernd H. A. Rehm*[,†,‡]

[†]Institute of Fundamental Sciences, Massey University, Private Bag 11222, Palmerston North, New Zealand

[‡]The MacDiarmid Institute for Advanced Materials and Nanotechnology, New Zealand

Supporting Information

ABSTRACT: In this study, fluorescent proteins (FPs) were engineered to self-assemble into protein particles inside recombinant *Escherichia coli* while mediating the display of various protein functionalities such as maltose binding protein or IgG binding domains of Protein A or G, respectively. *Escherichia coli* produced functional FP particles of up to 30% of cellular dry weight. The use of respective FP particles displaying certain binding domains in diagnostics and as bioseparation resins was demonstrated by direct comparison to commercial offerings. It was demonstrated that variable extensions (AVTS, FHKP, LAVG, or TS) of the N-terminus of FPs (GFP, YFP, CFP, HcRed) in combination with large C-terminal extensions such as translational fusion of the polyester synthase from *Ralstonia eutropha* or an aldolase from *Escherichia coli* led to extensive intracellular self-assembly of strongly fluorescent fusion protein particles of oval shape (0.5 × 1 μm). The strong fluorescent label of these bioparticles in combination with covalent display of protein functions provides a molecular toolbox for the design of self-assembled microparticles suitable for antibody-capture or ligand binding based diagnostic assays as well as the high affinity purification of target compounds such as antibodies.

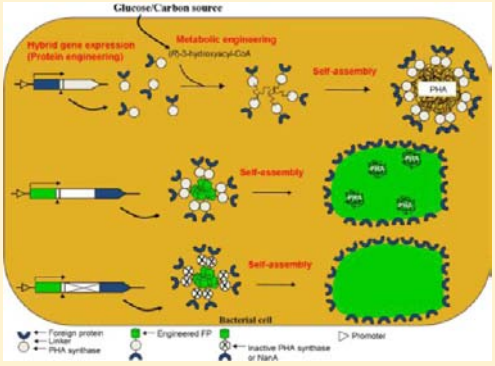

INTRODUCTION

The green fluorescent protein (GFP) is one of the most applied reporter proteins in modern science. It was discovered half a century ago when studying the chemiluminescence in the jellyfish *Aequorea aequorea*.[1] The intramolecular autocatalytic chromophore formation follows the folding of the protein and requires molecular oxygen to become fluorescent.[2,3] The enhanced yellow fluorescent protein (EYFP) and enhanced cyan fluorescent protein (ECFP) are GFP-derivatives derived from point mutations.[4,5] HcRed (HcR) is a dimeric red fluorescent protein derived from the Anthozoa species *Heteractis crispa*.[6]

GFP is widely used as a biological marker because it is known to not alter the function or localization of the targeted protein. GFP was fused to several aggregation-prone peptides, e.g., Alzheimer-related peptide Aβ42[7,8] or VP1 of the foot-and-mouth disease virus,[9−12] to investigate inclusion body formation and the amount of active, correctly folded fluorescent protein within these inclusion bodies. It was recognized that part of the inclusion bodies contained fully active protein.[13] Inclusion body formation was also observed and investigated for nonengineered GFP and it could be observed that the solubility of GFP is strongly dependent on its concentration.[14−16]

Polyhydroxybutyrate (PHB) serves as carbon and energy storage for bacteria in times of unbalanced growth. The key enzyme in the formation of the spherical insoluble PHB beads inside the cell is the PHB synthase PhaC.[17] Naturally, *Escherichia coli* does not produce PHB but can be genetically engineered for this purpose.[18−20] Upon overexpression of an engineered hybrid gene encoding the PhaC fused to a protein function of interest in the presence of excess carbon source PHB beads are formed inside *E. coli* cells. These beads can be isolated and stably maintained outside the bacterial cell displaying desired protein functionalities.[21]

Analysis of hybrid genes encoding GFP fused to PhaC revealed a possible alternative start codon upstream of the *gfp* gene that would N terminally extend GFP by four amino acids (AVTS). This extension was found to mediate protein aggregate formation as opposed to PHB bead assembly. In this study, the inherent property of FPs (fluorescent proteins) and variants to form fluorescent aggregates was harnessed by investigating whether fluorescent proteins can be engineered to self-assemble into protein particles displaying protein functions suitable for various applications in diagnostics or bioseparations.

EXPERIMENTAL PROCEDURES

Bacterial Strains, Growth Conditions, DNA Isolation, Analysis, and Manipulation. Bacterial strains and plasmids

Received: October 9, 2012
Revised: June 13, 2013
Published: July 8, 2013

   dx.doi.org/10.1021/bc300551j | *Bioconjugate Chem.* 2013, 24, 1314−1323

used in this study are listed in Supporting Information (SI) Table ST1, all primers used in this study are listed in SI Table ST2. General cloning procedures and isolation of DNA were performed as described elsewhere.[22] *E. coli* BL21(DE3) and XL1-Blue were grown at 25 or 37 °C, respectively. When required, ampicillin (75 μg/mL), chloramphenicol (50 μg/mL), and tetracycline (12.5 μg/mL) were added.

DNA sequences of new plasmid constructs were confirmed by DNA sequencing according to the chain termination method. All newly formed plasmids were used to transform competent *E. coli* BL21(DE3) cells and competent *E. coli* BL21(DE3) cells harboring plasmid pMCS69, which mediates the production of the precursor *R*-3-hydroxybutyryl-CoA for PHB synthesis.[23] A detailed description of each plasmid generation can be found in the SI.

Isolation of Polyester or Protein Inclusions and analysis. Protein particles were isolated from *E. coli* cultures following the protocol describing the isolation of polyester beads.[19] Gas chromatography/mass spectrometry (GC/MS) was used to analyze the PHB content of isolated cells.[24] Protein samples were analyzed by sodium dodecyl sulfate (SDS)-polyacrylamide gel electrophoresis (PAGE) as described elsewhere.[25] The gels were stained with Coomassie brilliant blue G250. The protein concentration was determined by the Bradford method.[26] Protein bands of interest were cut off the SDS polyacrylamide gel and analyzed by tryptic peptide fingerprinting applying collision induced dissociation tandem mass spectrometry (SI Table ST3). To identify the translation start, fusion proteins were subjected to N-terminal sequencing using Edman degradation.

Cells containing protein particles and isolated protein particles were examined for fluorescence as described previously.[27] For transmission electron microscopy (TEM) analysis, cells or beads were prepared as described previously.[18]

ELISA. Enzyme-linked immunosorbent assays were normalized according to protein concentration. The wells of microtiter plates were coated with 100 μL of a PHB bead or protein particle suspension and incubated overnight at 4 °C. After blocking and washing, the wells were incubated with either mouse monoclonal antibody to maltose binding protein (HRP) or antimouse IgG (HRP) conjugate for 1 h. After washing, substrate solution was added to each well and the substrate conversion was measured at 490 nm using a microtiter plate reader.

IgG Binding/Bioseparation. PHB beads as well as FP particles were tested for their ability to specifically bind and purify IgG from human serum. 50 mg of purified FP particles/PHB beads were sedimented (6000*g* for 4 min) and analyzed as described previously.[28] To assess binding of IgG using human IgG or goat IgG respectively as starting material, 50 mg beads/particles were sedimented and washed in PBS (10 mM KPO_4, 0.5% NaCl, pH 7.5), followed by incubation with IgG for 30 min at 25 °C. After sedimentation, beads/particles were washed three times in PBS and bound proteins were eluted with 50 mM glycine, pH 2.7. The elution fractions were analyzed with respect to total protein using the Bradford method and IgG as standard as well as with respect to protein composition using SDS-PAGE. A commercial offering (IPA300, Repligen, Waltham, MA, USA) was used for comparison.

Heat Inactivation. Protein particles were incubated in potassium phosphate buffer pH 7.4 for 30 min at each temperature. The temperature ranged from 50 to 80 °C and was increased in 10 °C steps.

Fluorescence Intensity Measurements. 50 mg wet drained FP particles were resuspended in 1 mL 50 mM potassium phosphate buffer, pH 7.5. 900 μL of the suspension was loaded onto the cuvette for scanning in a spectrofluorometer (HORIBA Scientific Fluoromax-4NIR Spectrofluorometer, FluorEssence software; Kyoto, Japan). ECFP derivatives were analyzed using an excitation maximum of 433 nm and an emission maximum of 475 nm with a 2.5 nm slit. EYFP derivatives were scanned with an excitation maximum of 511 nm and an emission maximum of 526 nm with a 1.5 nm slit. GFP particles were analyzed using an excitation maximum of 457 nm and an emission maximum of 519 nm with a 1 nm slit, and HcR derivatives were analyzed using an excitation maximum of 587 nm and an emission maximum of 637 nm with a 5 nm slit. The slit widths were chosen according to the emission wavelengths.

Immunochromatographic Strips. FP particles (1.6 mg/mL) were sonicated for 10 min, followed by washing in PBS and incubation with antisteroid antibody on a rocker for 30 min at room temperature. After centrifugation the antibody coated particles were resuspended in bead buffer (per 50 mL, pH 7.4: 0.35 g Na_2HPO_4, 0.05 g casein hydrolysate, 0.05 g sodium azide; filtered through a Millipore HAWP 0.45 μm membrane, stored at 4 °C).

Nitrocellulose membrane (Millipore FF75; EMD Millipore, Billerica, MA, USA) was sprayed at 1.008 μL/cm with a capture material consisting of a 1 mg/mL solution of steroid-bovine serum albumin conjugate and dried for one hour at 37 °C (Biodot XYZ 3200; Biodot, Irvine, CA, USA). The commercial cards had the lower 20 mm portion removed using a guillotine. The strips were then cut to 5 mm widths using the Biodot CM4000.

An assay mixture was prepared consisting of particles (110 μL, diluted 1/50 in bead buffer), antisteroid monoclonal antibody, and buffer (330 μL; 100 mM NaCl, 0.4% Tween-20, 0.8% polyvinyl pyrrolidone in 50 mM phosphate buffer, pH 7.4, containing 1% BSA). The assay mixture was placed into each well with either a zero standard or one of a series of standard solutions of steroid designed to cover the standard curve working range. After 15 min the strips were scanned on a FLA-5000 scanner (Fujifilm, Tokyo, Japan).

RESULTS

Engineering of GFP toward *in Vivo* Self-Assembly of Bioparticles. GFP was N-terminally extended by four amino acid residues (M)AVTS and its C-terminus was extended by the polyester synthase (encoded by *phaC* from the bacterium *Ralstonia eutropha*), an insolubility protein partner,[18] which mediates the formation of insoluble PHB inclusions inside recombinant bacteria.[29] While the non-N-terminally extended GFP fused to PhaC led to the formation of PHB contributing to about 35% of bacterial biomass, the engineered extGFP-PhaC mediated only the synthesis of PHB contributing to about 8% of the bacterial biomass. N-terminal sequencing of the engineered GFP fusion protein confirmed an extension of four amino acid residues ((M)AVTSMS).

To assess the applicability of GFP particles for the display of foreign protein functions, a hybrid gene encoding the extGFP-PhaC-linker-MalE fusion protein was constructed and overexpressed. Recombinant *E. coli* cells overproducing this FP fusion protein did not show any PHB production, as was confirmed by GC/MS analysis. FP fusion protein particles could be isolated from these cells by using a two-step glycerol density gradient

ultracentrifugation (Figure 1A) and were visualized by TEM as homogeneous electron scattering particles (0.5 × 1 μm)

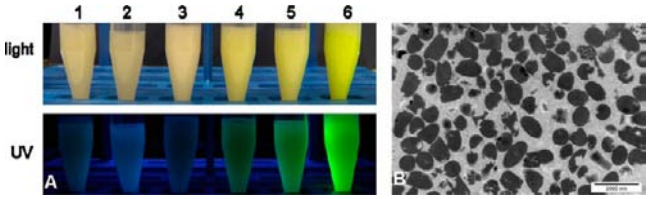

Figure 1. Fluorescence of FP particles and producing *E. coli* cultures as well as FP particle morphology. A. Lane 1, *E. coli* BL21(pMCS69/pET-14b GFP-PhaC-linker-MalE); lane 2, *E. coli* XL1-Blue(pBHR69 gfp-phaC); lane 3, *E. coli* XL1-Blue(pMCS69/pCWE extGFP-PhaC-linker-MalE); lane 4, *E. coli* BL21(pMCS69/pET-14b extGFP-PhaC-linker-MalE); lane 5, *E. coli* BL21(pET-14b extGFP-PhaC-linker-MalE); lane 6, FP particles isolated from 4 in suspension. B. TEM image of the isolated FP particles derived from *E. coli* BL21(pMCS69/pET-14b extGFP-PhaC-linker-MalE).

without PHB inclusions (Figure 1B). The fusion partner MalE (MBP = maltose binding protein) could be detected as displayed at the protein particle surface by ELISA using HRP-labeled anti-MalE antibodies (SI Figure S1). The same plasmid but containing a mutated *phaC* encoding an inactive polyester synthase in which the active site cysteine 319 − which is essential for activity[30] − was replaced by alanine, also resulted in FP fusion protein particle formation (data not shown). Cells producing the nonextended GFP fusion encoded by pET-14b GFP-PhaC-linker-MalE produced PHB beads. These cultures did not show any green fluorescence and produced fusion protein displaying PHB beads instead of FP fusion protein particles (Figure 2).

Exchange of the Functional Fusion Partners to Demonstrate Broader Applicability of the GFP-PhaC Protein Particles. MalE was replaced by the IgG binding domain ZZ of Protein A (extGFP-PhaC-linker-ZZ) and a single (extGFP-PhaC-linker-GB1) as well as a triple repeat of the IgG binding domain of Protein G (extGFP-PhaC-linker-SG-[GB1]3) (SI Figure S2). Cells overproducing the fusion proteins, respectively, showed PHB synthesis when the PhaC synthase substrate (*R*)-3-hydroxybutyryl-CoA was metabolically provided (Figure 2). In the absence of PhaC substrate or when inactive PhaC was part of the fusion protein, PHB could not be detected and cells efficiently produced GFP protein particles (22−30% wet FP particles mass/wet biomass). In the presence of PhaC substrate the extGFP-PhaC-linker-[GB1]3 fusion protein mediated PHB bead formation, while fusion proteins extGFP-PhaC-linker-ZZ or extGFP-PhaC-linker-GB1 mediated the formation of FP/PHB hybrid particles as shown by TEM (Figure 3A). PHB beads, protein particles, and the hybrid particles displayed the respective ZZ or (GB1)3 binding domains as assessed by ELISA, and they enabled purification of IgG from pooled human serum using a batch bind and elute bioseparation method (Figures 3B, C, SI Figures S3, S4). PHB beads, hybrid particles, as well as protein particles displaying either a single or triple repeat of the GB1 domain were also subjected to IgG purification assays using goat serum as source, which IgG should specifically bind to the Protein G derived GB1 domain (SI Figure S5). Generally, protein particles and hybrid particles showed strongly increased IgG binding capacity when compared to respective PHB beads and a commercial

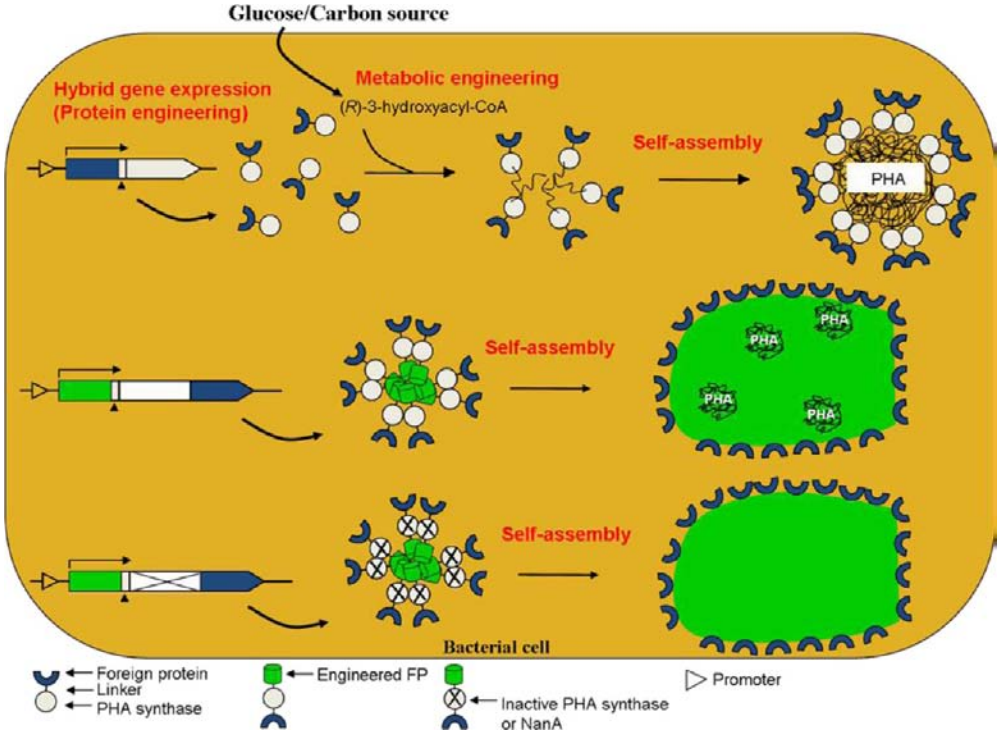

Figure 2. Schematic overview of PHB bead and FP particle formation described in this study. Upon *phaC* gene expression and availability of a suitable carbon source PHB beads are synthesized inside engineered *E. coli* cells (top). The expression of hybrid genes comprising extended GFP, PhaC, and either ZZ or GB1 leads to the self-assembly of a FP-PHB hybrid (middle). The expression of hybrid genes comprising an extended FP, mutated PhaC (depicted by the cross in the wide box), and a C-terminal fusion partner (e.g., triple repeat of GB1) leads to the self-assembly of strongly fluorescent FP particles inside *E. coli* (bottom). All three particle varieties described above display functional surface protein domains.

dx.doi.org/10.1021/bc300551j | *Bioconjugate Chem.* 2013, 24, 1314−1323

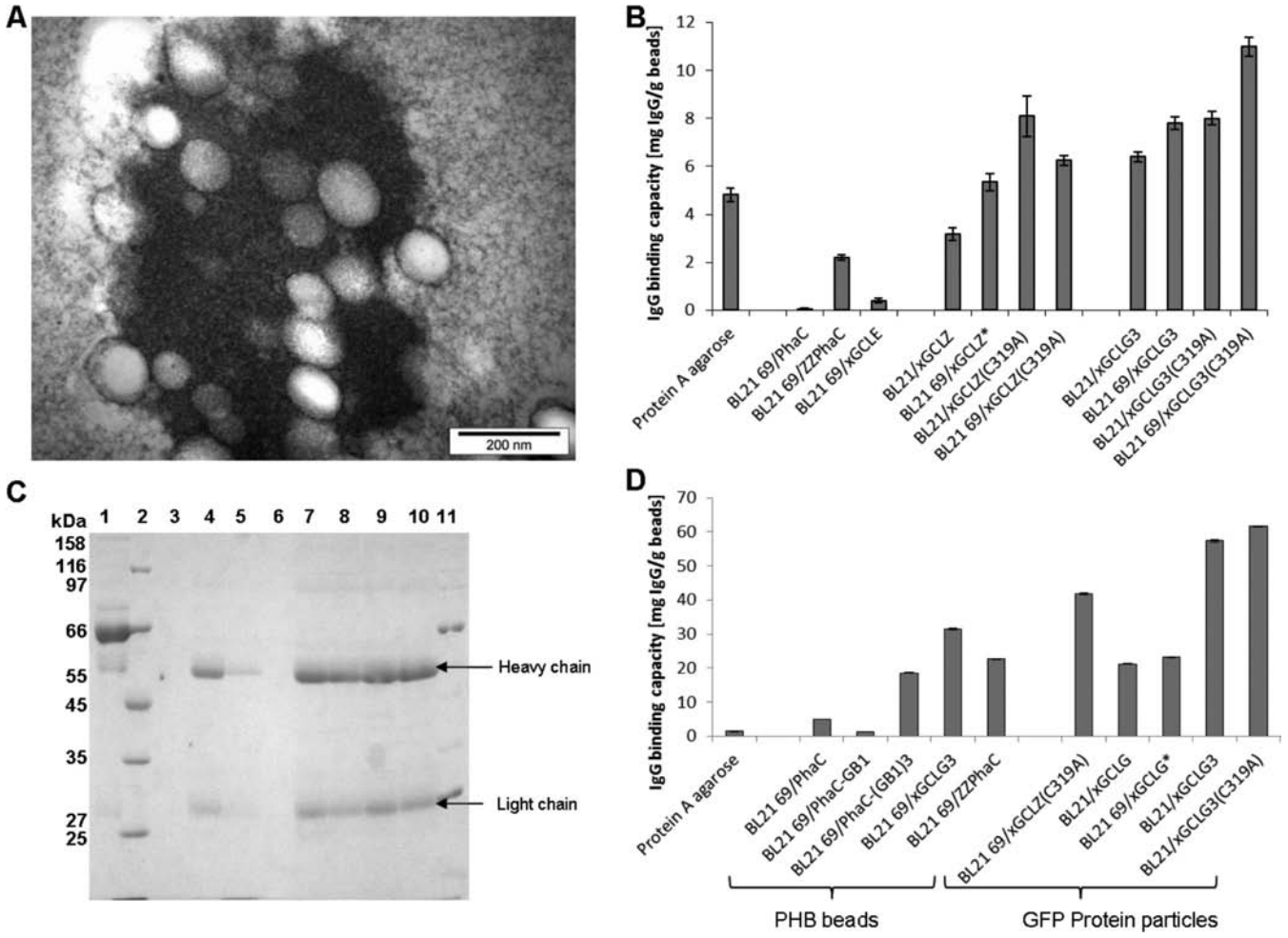

Figure 3. A. TEM image of isolated PHB/FP hybrid material produced by *E. coli* BL21(pMCS69/pET-14b extGFP-PhaC-linker-GB1). B. IgG binding capacity of various FP particles in a bioseparation assay using human serum. The protein concentration was measured by the Bradford method using purified IgG as standard; 50 mg beads were used for the assay and the binding capacity was compared to 100 μL bed volume of Protein A agarose (IPA300, Repligen, Waltham, MA, USA). All measurements were conducted in triplicate and the standard deviation is indicated. A star indicates PHB/protein hybrid material. All particles were produced in either BL21 or BL21(pMCS69) harboring the respective pET-14b plasmid (BL21/; BL21 69/). BL21 69/PhaC, PhaC PHB beads; BL21 69/ZZPhaC, ZZPhaC PHB beads; BL21 69/xGCLE, extGFP-PhaC-linker-MalE FP particles; BL21 69/xGCLZ, extGFP-PhaC-linker-ZZ FP/PHB hybrid; BL21 69/xGCLZ(C319A), extGFP-PhaC(C319A)-linker-ZZ FP particles; BL21 69/xGCLG3, extGFP-PhaC-linker-[GB1]3 PHB beads; BL21 69/xGCLG3(C319A), extGFP-PhaC(C319A)-linker-[GB1]3 FP particles. C. SDS-PAGE showing IgG purification results. D. Goat IgG binding capacity. The assay was performed as described in B, except that goat IgG was used for standardization. Abbreviations as in B; BL21 69/PhaC-(GB1)3, PhaC-[GB1]3 PHB beads; BL21 69/xGCLGB1, extGFP-PhaC-linker-GB1 FP/PHB hybrid; BL21/xGCLG, extGFP-PhaC-linker-GB1 FP particles.

offering. In addition, increased IgG binding depending on the number of GB1 repeats could be observed (Figure 3D).

C-Terminal Fusion of a Protein Is Required to Enable Self-Assembly of N-Terminally Extended GFP. Only the gene encoding GFP and the extended GFP was overexpressed under the control of the strong T7 promoter. Cultures of *E. coli* BL21(DE3) cells harboring the respective plasmids were fluorescent, but after cell disruption, the fluorescence, i.e., the GFP, was found in the soluble fraction (data not shown). The same applied to cells overproducing GFP-GB1 or extGFP-GB1. Analysis of cells overproducing GFP-L-SG-[GB1]3, extGFP-L-SG-[GB1]3, GFP-ZZ, or extGFP-ZZ, respectively, showed that the majority of the FP fusion protein resided in the soluble fraction (data not shown). To assess whether PhaC is specifically required for self-assembly of extGFP particles, PhaC was replaced by the cytosolic soluble enzyme NanA (N-acetylneuraminate lyase from *E. coli*[31]) and the formation of GFP particles was assessed. Cells overproducing extGFP-NanA-linker-ZZ produced GFP particles similar in size and morphology when compared to particles made of extGFP-PhaC-linker-MalE (see Figure 1B). Human serum was used to assess the IgG purification performance and the binding capacity of the respective protein particles which resulted in a comparable purification of IgG and an about 3.5-fold greater binding capacity when compared to commercially offered recombinant protein A cross-linked agarose beads (Figure 4A, SI Figure S6). As both PhaC and NanA can form oligomers, an additional control fusion protein comprising MalE as central fusion partner was designed. Both GFP-MalE-linker-ZZ as well as extGFP-MalE-linker-ZZ were overproduced in *E. coli* cells and led to the formation of GFP particles. Particles comprising extended GFP fusion protein showed brighter fluorescence and a slightly increased IgG binding capacity compared to the nonextended version (SI Figure S7). Also, the proximity between GFP and its C-terminal fusion partner, which might have impaired independent folding of PhaC, was assessed by

dx.doi.org/10.1021/bc300551j | *Bioconjugate Chem.* 2013, 24, 1314−1323

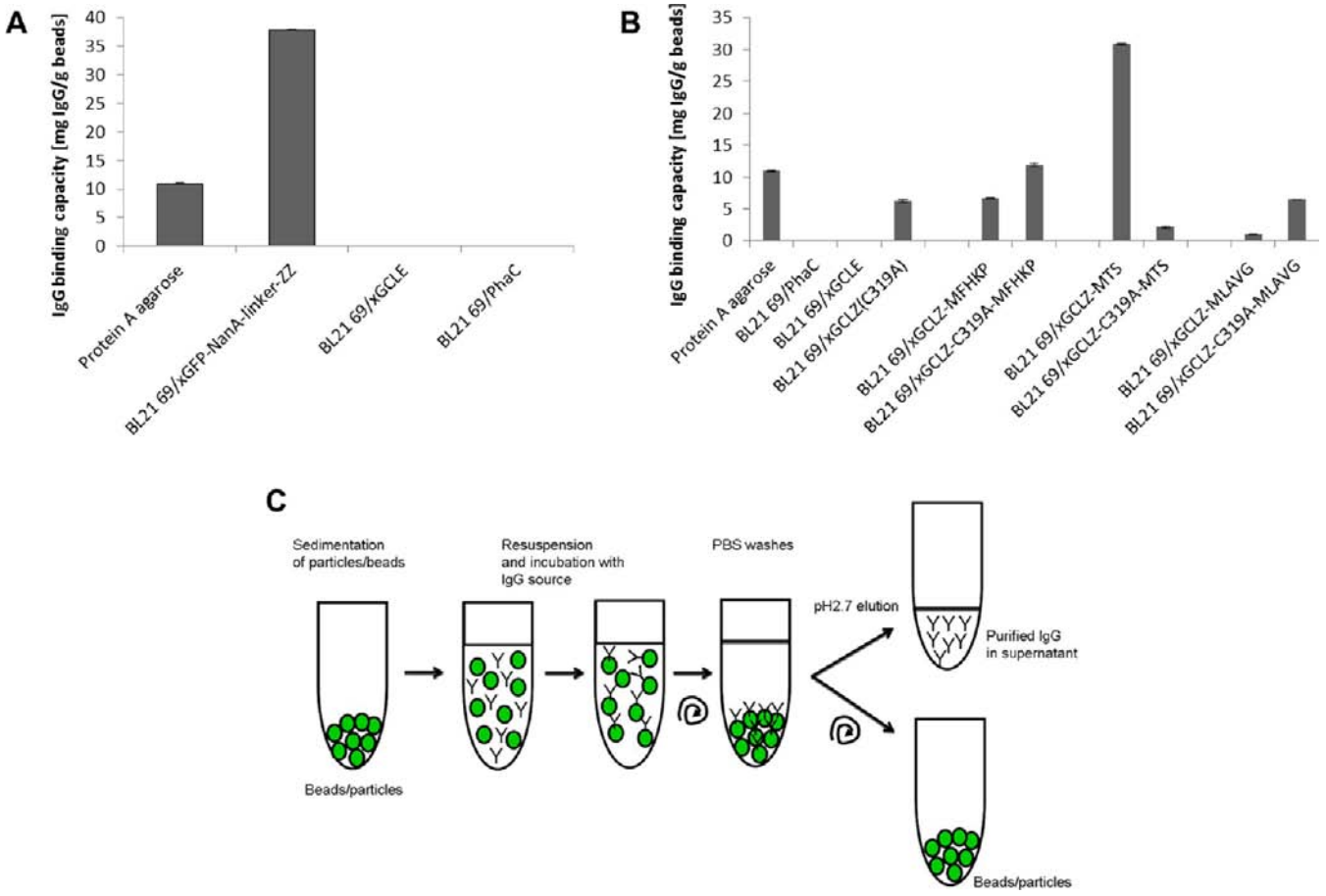

Figure 4. A. IgG binding capacity in a bioseparation assay using human serum. Abbreviations as previously stated. BL21 69/xGFP-NanA-linker-ZZ, FP particles derived from *E. coli* BL21 (pMCS69/pET-14b extGFP-NanA-linker-ZZ). Readings for BL21 69/xGCLE and BL21 69/PhaC were 0. B. The impact of various N-terminal extensions on FP particle performance. The IgG binding capacity was assessed as the amount of eluted IgG protein compared to commercial Protein A agarose (IPA300, Repligen, Waltham, MA, USA) using beads showing MFHKP, MLAVG, or MTS extension. The protein concentration was determined by the Bradford method. All measurements were conducted in triplicate and the standard deviation is indicated. Abbreviations as previously stated. BL21 69/xGCLZ-MFHKP, extGFP(MFHKP)-PhaC-linker-ZZ PHB beads; BL21 69/xGCLZ-C319A-MFHKP, extGFP(MFHKP)-PhaC(C319A)-linker-ZZ FP particles; BL21 69/xGCLZ-MTS, extGFP(MTS)-PhaC-linker-ZZ PHB beads; BL21 69/xGCLZ-C319A-MTS, extGFP(MTS)-PhaC(C319A)-linker-ZZ FP particles; BL21 69/xGCLZ-MLAVG, extGFP(MLAVG)-PhaC-linker-ZZ PHB beads; BL21 69/xGCLZ-C319A-MLAVG, extGFP(MLAVG)-PhaC(C319A)-linker-ZZ FP particles. C. Schematic overview of the batch bind and elute IgG purification/bioseparation used in this study.

inserting a pentaglycine linker between GFP and PhaC which resulted in the fusion protein GFP-G5-PhaC-linker-ZZ and the respective extended version. *E. coli* cells overproducing these fusion proteins produced GFP particles which were able to purify IgG but showed a lower IgG binding capacity than particles without the pentaglycine linker (SI Figure S7).

Importance of a Defined N-Terminal Extension of GFP for GFP Particle Formation. Different extensions of the GFP protein were tested for their ability to promote the formation of GFP particles. Two extensions had the same length as the original one but displayed different amino acids ([M]LAVG and [M]FHKP). A third extension tested was shorter but displayed the last two amino acids of the original extension ([M]TS). Each extension was tested with a set of four FP fusion proteins, expressing either active or inactive synthase in combination with the two reporter proteins, ZZ or MalE. The expression of each hybrid gene was assessed in the presence and absence of PhaC substrate. In summary, production of the respective fusion proteins comprising an active PhaC in the presence of substrate always led to the formation of PHB beads, which was independent of the individual extension. However, in the absence of PhaC substrate, protein particles were formed but showed varying levels of fluorescence and activity (SI Figures S8, S9, S10). In the absence of PhaC substrate FP particles comprising one of the two four-amino-acid extensions (FHKP, LAVG) and the reporter protein ZZ were often nonfluorescent. FP particles comprising one of the two aforementioned extensions and MalE mostly showed fluorescence. The level of fluorescence could not be correlated with the activity of the reporter protein (Figure 4B) when assessed by a batch bind and elute method (Figure 4C).

Characterization of the GFP Particle Formation and Composition. When cells were cultured at 37 °C, nonfluorescent FP particles were produced whereas culturing at 25 °C led to the formation of fluorescent FP particles. FP protein particles were isolated from cells grown under different cultivation temperatures, and no difference in the protein profile was observed when particles were assessed by SDS-PAGE analysis (data not shown). Under anaerobic culture conditions at 25 °C, no fluorescence of FP particles could be observed. GFP particles isolated from cells grown aerobically at 25 °C were susceptible to heat inactivation. Incubation at 80 °C

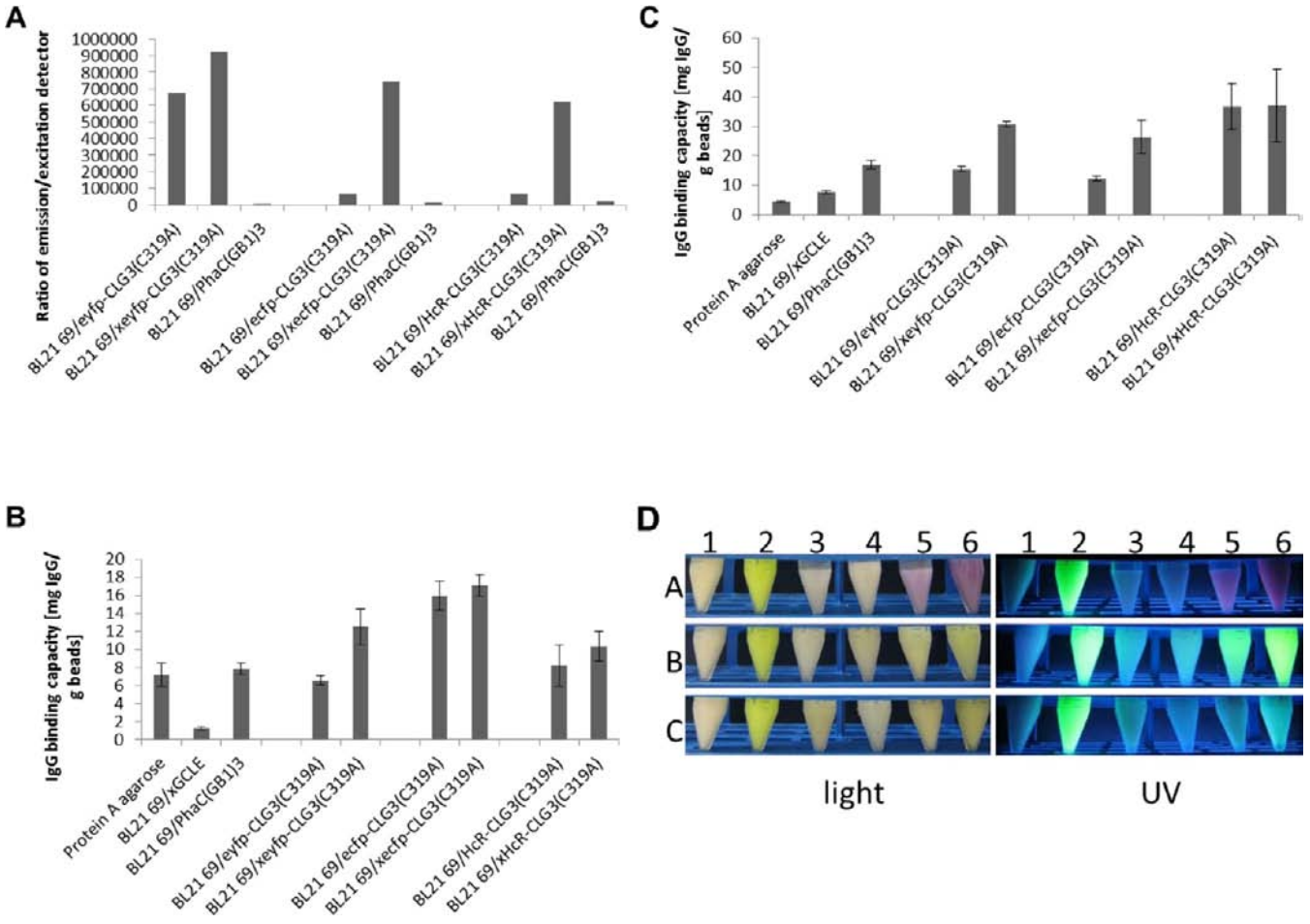

Figure 5. Comparative analysis of various FP particles with respect to fluorescence intensity and IgG binding capacity. Abbreviations as previously stated. A. Fluorescence intensities of FP particles (x = MAVTS extension). BL21 69/eyfp-CLG3(C319A), eyfp-PhaC(C319A)-linker-[GB1]3 FP particles; BL21 69/xeyfp-CLG3(C319A), xeyfp-PhaC(C319A)-linker-[GB1]3 FP particles; BL21 69/ecfp-CLG3(C319A), ecfp-PhaC(C319A)-linker-[GB1]3 FP particles; BL21 69/xecfp-CLG3(C319A), xecfp-PhaC(C319A)-linker-[GB1]3 FP particles; BL21 69/HcR-CLG3(C319A), HcR-PhaC(C319A)-linker-[GB1]3 FP particles; BL21 69/xHcR-CLG3(C319A), xHcR-PhaC(C319A)-linker-[GB1]3 FP particles. B. Human IgG (serum) binding capacities of FP particles. C. IgG3 (goat IgG) binding capacities of FP particles. Measurements displayed in B and C were conducted in triplicate; the respective standard deviations are indicated. D. Fluorescence of FP particles in normal light (left) and UV light (right). Panel A is showing HcR and xHcR particles, panel B is displaying eyfp and xeyfp particles, and panel C is picturing ecfp and xecfp particles. Lane 1, PHB beads derived from *E. coli* BL21(pMCS69/pET-14b PhaC); lane 2, GFP particles from *E. coli* BL21(pMCS69/pET-14b extGFP-PhaC-linker-MalE); lane 3, nonextended FP particles from *E. coli* BL21(pET-14b FP-PhaC-linker-[GB1]3); lane 4, nonextended FP particles from *E. coli* BL21(pMCS69/pET-14b FP-PhaC-linker-[GB1]3); lane 5, MAVTS extended FP particles from *E. coli* BL21(pET-14b extFP-PhaC-linker-[GB1]3); lane 6, MAVTS extended FP particles from *E. coli* BL21(pMCS69/pET-14b extFP-PhaC-linker-[GB1]3).

for 30 min abolished fluorescence (SI Figure S11). To verify the proteinaceous nature of the particles, they were also incubated with Proteinase K and solubilized in 8 M Urea. These treatments resulted in complete degradation and solubilization, respectively, of the GFP particles as well as the concomitant loss of fluorescence (data not shown).

Influence of the N-Terminal Tetrapeptide AVTS on Self-Assembly of Various FPs. The enhanced yellow FP (EYFP), enhanced cyan FP (ECFP), and far red FP HcRed (HcR) were also engineered to contain the originally identified N-terminal four amino acid residues (AVTS). For proof-of-concept, protein fusions comprising the triple repeat of the IgG binding domain GB1 fused to the C-terminus of the inactive synthase PhaC(C319A) were designed with N-terminally fused either nonextended or extended FP (SI Figure S12). Each FP fusion protein mediated the formation of the respective protein particles, independent of PhaC substrate. Protein particles comprising the extended versions always showed visible color, enhanced fluorescence intensities, and better performance in IgG binding, i.e., greater IgG binding capacity when compared to particles comprising nonextended fusion protein (Figure 4, SI Figures S13, S14). Due to the fusion partner – a triple repeat of the GB1 domain – all particles showed superior binding capacities for IgG of the subclass 3 as opposed to IgG from pooled human serum. Protein particles comprising the extended FPs ECFP or EYFP showed a greater difference when compared to their nonextended versions than the respective particles made of HcRed, where extended and nonextended protein particles behaved very similar with respect to IgG binding. Generally, FP particles comprising any extended fusion protein showed a 1.5–2-fold greater IgG_3 binding capacity when compared to respective PHB beads (e.g., PhaC(GB1)3).

Application of Functionalized FP Particles in Bioseparation and Immunochromatographic Strips. Human serum albumin is the most abundant protein in human blood

dx.doi.org/10.1021/bc300551j | *Bioconjugate Chem.* 2013, 24, 1314–1323

serum preparations and purification of Ig antibodies is often desirable for various diagnostic and medical applications. FP particles designed in this study were tested in a batch and elute bioseparation assay using human serum for their applicability as specific and high-affinity IgG bioseparation matrix. This assay was also employed to determine the specific IgG binding capacity compared to a commercial Protein A agarose offering. SI Figures S4 and S13 highlight the purification power of the respective FP particles displaying IgG binding domains of Protein A or G, respectively, at the particle surface. A clear enrichment of the heavy and light chain of IgG is visible in the elution fractions compared to the human serum loading control. All FP particles showed a 2−6-fold greater IgG binding capacity in the bioseparation assay using human serum when compared to a commercial Protein A offering (Figures 3B, 4A, 5B).

Nanogold is regarded as standard label for lateral flow. The respective antibodies are passively adsorbed to the nanogold using standard procedures (Figure 6A). Here, the utility of FP particles made of extGFP-PhaC(C319A)-linker-ZZ, i.e., GFP particles displaying the Protein A derived IgG binding ZZ domain, in immunochromatographic strip analysis was investigated. An anti-steroid monoclonal antibody was immobilized to the FP particles via the displayed Z domains. FP particles coated with anti-steroid monoclonal antibody were subjected to varying concentrations of the steroid. The strip assay works in analogy to common pregnancy tests as a competitive assay. The FP particles were subjected to immunochromatographic strip membranes and bound to the strip-immobilized steroid. The particles were able to migrate inside the modified nitrocellulose membrane, and binding to the immobilized steroid was detected by fluorescence scanning. A decrease in fluorescence intensity, due to fewer bound FP particles, was obtained as a function of increasing steroid concentration (Figure 6B,C). Nanogold as well as FP particles showed similar EC50 values within the experimental error (91.1 mg/mL for FP particles, 102.1 mg/mL for nanogold). The FP particles showed a wider working range for the detection of the steroid molecule from approximately 10−1000 ng/mL, whereas nanogold showed a working range from 30 to 500 ng/mL.

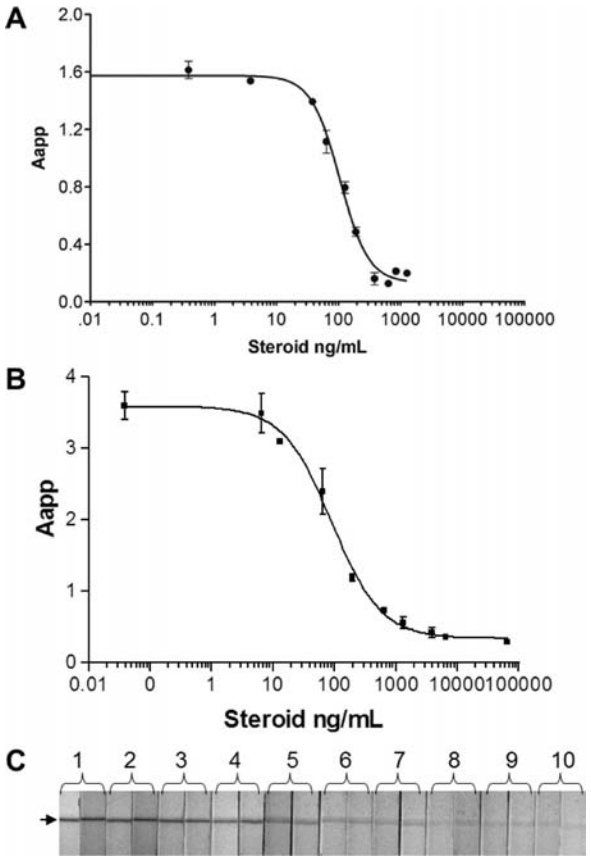

Figure 6. Application of fluorescent particles in immunochromatographic strips measuring steroid concenctrations. A. Steroid standard curve using gold nanoparticles (40 nm, Diagnostic Consulting Network, CA, USA). B. Standard curve of the immunochromatographic strip assay using FP particles. Aapp, arbitrary fluorescence intensity unit. C. Strips used in B showing a decrease in fluorescence intensity as a function of increasing steroid concentration (left to right). Strips were shown as duplicates; numbers indicate measured concentrations as depicted in B with 1 showing the result for the lowest steroid concentration.

DISCUSSION

GFP is a fluorescent reporter protein widely used in modern research laboratories.[32−36] In this study, GFP was initially employed to investigate whether the polyester synthase PhaC could serve as a self-assembly promoting fusion partner for the formation of protein particles suitable for applications such as bioseparations and diagnostics.

Previous studies using GFP as a reporter fused to the N terminus of PhaC showed no negative influence or inactivation of the synthase protein.[27,37,38] N-terminally extended GFP versions only self-assembled when overproduced by using the strong T7 promoter.[39] This is in agreement with studies finding GFP inclusion body formation after expression from a strong promoter.[14,15,40] Recent studies reported the intrinsic capability of the R9 peptide, comprising nine arginine residues, to cause GFP self-organization.[41] All these studies were conducted with plain GFP[14,15,40] or GFP having fused only a short sequence additionally to the N- or C-terminus.[41]

In this study, the use of an alternative start codon resulted in the production of the four-amino-acid residue N-terminally extended GFP. These four additional amino acids altered the properties of the GFP when fused to PhaC and when produced from the strong T7 promoter, which resulted in the production of protein particles instead of PHB inclusions (Figure 1). These protein particles could not be detected in control experiments overproducing only GFP and extGFP, suggesting that the C-terminal PhaC fusion partner was required for the self-assembly process. To exclude the possibility that self-assembly is promoted by the formation of small PHB granules due to PhaC activity, an inactive modified PhaC was used, which also led to protein particle formation. These data suggested that the PhaC activity did not initiate protein bead self-assembly, but presumably the protein itself contributed to the self-assembly due to its structural properties which cause it to form oligomers.[42] Further investigation showed that PhaC can be replaced by another protein, NanA (randomly chosen soluble cytosolic enzyme), without impairing the formation of GFP particles. These findings together with the results obtained for direct GFP and ext-GFP fusions suggested that the presence of a C-terminal fusion partner does have impact on the formation of protein particles rather than the activity of the actual fusion partner itself. However, it should be mentioned here that both fusion partners, PhaC and NanA, form homooligomers and this inherent property could have attributed to the aggregation

Table 1. Summary of the Properties of Constructs Evaluated in This Study

N-terminal peptide	fluorescent protein species	C-terminal fusion partner	displayed functionality	PHB content	fluorescence strength
-	GFP	PhaC	-	+	-
AVTS	GFP	PhaC	-	+	-
-	GFP	PhaC-linker-	MalE	+	-
AVTS	GFP	PhaC-linker-	MalE	-	++
AVTS	GFP	PhaC-linker-	ZZ/GB1	+*	++
AVTS	GFP	PhaC-linker-	(GB1)3	+	-
AVTS	GFP	PhaC(C319A)-linker-	ZZ/GB1/(GB1)3	-	++
AVTS	GFP	NanA-linker-	ZZ	-	++
LAVG/FHKP/MTS	GFP	PhaC-linker-	MalE/ZZ	+	+
LAVG/FHKP/MTS	GFP	PhaC(C319A)-linker-	MalE/ZZ	-	+
-	EYFP/ECFP/HcR	PhaC(C319A)-linker-	(GB1)3	-	-
AVTS	EYFP/ECFP/HcR	PhaC(C319A)-linker-	(GB1)3	-	++

process. Hence to assess the role of the fusion partner in self-assembly, the monomeric soluble protein, MalE, was used as fusion partner. Fusion proteins of GFP or xGFP fused to MalE, respectively, mediated formation of FP particles but showed lower binding activity than particles comprising PhaC or NanA. The same was observed for particles formed by fusion proteins comprising an additional pentaglycine between GFP and the C-terminal fusion partner. As all these proteins are produced in a high concentration, random inclusion body formation cannot be excluded. Nevertheless, all particles comprising extended GFP fusion protein showed brighter fluorescence and higher activity. An additional fusion of MalE to the C terminus of PhaC resulted in the fusion protein extGFP-PhaC-linker-MalE which mediated the formation of strongly fluorescent protein particles displaying the functional MalE protein and indicating that the protein particles can be functionalized and used for the surface display of proteins. Further functionalization of the protein particles was achieved by exchanging the fusion partner MalE with the IgG binding domains of protein A or protein G, respectively. These GFP particles successfully purified IgG from human serum and showed up to 3.5-fold greater binding capacity than commercial Protein A beads used as control (Figures 3B, 4A). Protein beads engineered to bind IgG of the human IgG subclass 3 showed specific binding as assessed by goat IgG binding (Figure 3D).

In contrast to protein particles displaying MalE, which were always negative for PhaC activity, three of the IgG binding domain displaying particles were made of PHB (extGFP-PhaC-linker-[GB1]3) or at least consisted partially of PHB (extGFP-PhaC-linker-ZZ, extGFP-PhaC-linker-GB1). The domains GB1 and ZZ seemed to enhance solubility[43,44] and compete with the N-terminal GFP extension with respect to GFP particle self-assembly but still enabled the PHB synthesis based self-assembly of PHB inclusions. Further investigation into the cross-talk between these two protein regions that presumably interfere with the extended GFP mediated self-assembly would be necessary and are required to understand the mechanism of this self-organization process. However, when inactive PhaC or NanA were used as a linker region between GFP and the binding domain (GB1 or $[GB1]_3$ or ZZ) then only fluorescent protein particles with the respective protein functionality were obtained.

The GFP particles were characterized and heat sensitivity data as well as the requirement of oxygen suggested that the extended GFP showed properties as described for GFP.[2,3,45,46] In a previous study, targeted GFP inclusion body formation showed that this protein remains active and fluorescent in insoluble particles.[9,11,16] These findings were confirmed by data obtained in this study, although the inclusion body formation was not induced by a specific sequence, i.e., an insolubility tag, rather than by an N-terminal extension of GFP itself and a C-terminal fusion. Different N-terminal extensions were investigated regarding their ability to induce the formation of GFP particles. Although all of the tested extensions caused the formation of GFP particles, none could overrule the PhaC polyester bead formation activity when substrate was provided as observed with the original extension AVTS.

Three other FPs, ECFP, EYFP, and HcR, were assessed for their susceptibility to (M)AVTS extension mediated self-assembly. As shown with GFP, N-terminally extended versions of the three fluorophores showed brighter color and greater fluorescence intensity than their nonextended counterparts (Figure 5A,D). Similarly, particles derived from extended FP fusion proteins showed better performance regarding human and goat IgG binding capacities (Figure 5B,C). ECFP and EYFP are nearly sequence identical with GFP and HcR also shares approximately 21% amino acid sequence identity with GFP and forms a β-barrel structure comparable to GFP and its derivatives.[6,47]

In this study, cells were engineered to strongly overproduce FPs by expression from a strong promoter. In addition, FP particle formation was in agreement with previous findings describing that growth conditions influence solubility of recombinant proteins expressed in *E. coli*,[8,14] i.e., higher growth temperatures and long incubation times favor the production of insoluble protein inclusions.

The yield of the FP microparticles of up to 30% over biomass suggested that these new fluorescent functional materials could be cost-effectively produced when considered as affinity bioseparation resins or for diagnostic applications.

CONCLUSIONS

Overall, this study demonstrated that overproduction of an N-terminally extended FP, not only when fused to PhaC as a self-assembly promoting fusion partner but also when fused to a soluble enzyme, enabled the efficient production of fluorescent FP particles. Furthermore, C-terminal fusions did not interfere with FP particle assembly and enabled the functional display of foreign proteins (Table 1). The N-terminal extension (M)AVTS was found to be superior over other tested extensions. The particle formation was not limited to extended GFP but could also be observed with the GFP-like FPs EYFP and ECFP, as well as with HcR. Generally, FP particles derived from (M)AVTS extended FPs showed enhanced fluorescence

intensity and performance. These strongly fluorescent particles with an intrinsic label can be tailored to covalently display proteins for applications in antibody capture-based diagnostic assays, e.g., immunochromatographic strips (Figure 6) or for batch bind-and-elute bioseparation applications. The modular arrangement of the protein domains provides a large design space for the production of custom-made fluorescent materials.

■ ASSOCIATED CONTENT

Supporting Information

A detailed description of the cloning procedure. Table ST1 lists all strains and plasmids used in this study, ST2 lists all primers and ST3 MALDI-TOF/MS results. Figures illustrate ELISA, SDS-PAGE, and heat inactivation results. This material is available free of charge via the Internet at http://pubs.acs.org.

■ AUTHOR INFORMATION

Corresponding Author

*Phone: +64 6 350 5515 ext 7890; fax: +64 6 350 2267; e-mail: b.rehm@massey.ac.nz.

Present Address

Anika Jahns, Department of Medical Biosciences/Pathology, Umeå University, Sweden. Yogananda Maspolim, Nanyang Environment and Water Research Institute (NEWRI), Nanyang Technological University N1−B3b-29, Singapore.

Notes

The authors declare no competing financial interest.

■ ACKNOWLEDGMENTS

This work was supported by the New Zealand Foundation for Research Science and Technology, Massey University Research Fund, and the MacDiarmid Institute of Advance Materials and Nanotechnology. Dr. Anika Jahns received a Technology for Industry Doctoral Fellowship. This research has been facilitated by access to the Australian Proteome Analysis Facility established under the Australian Government's Major National Research Facilities program. Dr. Indira Rasiah is acknowledged for constructing the plasmid pET-14b gfp-phaC. Mrs. Jane Mullaney is acknowledged for constructing the plasmid pET-14b PhaC-linker-ZZ.

■ REFERENCES

(1) Shimomura, O., Johnson, F. H., and Saiga, Y. (1962) Extraction, purification and properties of aequorin, a bioluminescent protein from the luminous hydromedusan *Aequorea*. *J. Cell Comp. Physiol. 59*, 223−239.

(2) Heim, R., Prasher, D. C., and Tsien, R. Y. (1994) Wavelength mutations and posttranslational autoxidation of green fluorescent protein. *Proc. Natl. Acad. Sci. U. S. A. 91*, 12501−12504.

(3) Reid, B. G., and Flynn, G. C. (1997) Chromophore formation in green fluorescent protein. *Biochemistry 36*, 6786−6791.

(4) Tsien, R. Y. (1998) The green fluorescent protein. *Annu. Rev. Biochem. 67*, 509−544.

(5) Stuurman, N., Pacios Bras, C., Schlaman, H. R. M., Wijfjes, A. H. M., Bloemberg, G., and Spaink, H. P. (2000) Use of green fluorescent protein color variants expressed on stable broad-host-range vectors to visualize rhizobia interacting with plants. *Mol. Plant-Microbe Interact. 13*, 1163−1169.

(6) Gurskaya, N. G., Fradkov, A. F., Terskikh, A., Matz, M. V., Labas, Y. A., Martynov, V. I., Yanushevich, Y. G., Lukyanov, K. A., and Lukyanov, S. A. (2001) GFP-like chromoproteins as a source of far-red fluorescent proteins. *FEBS Lett. 507*, 16−20.

(7) de Groot, N. S., and Ventura, S. (2006) Protein activity in bacterial inclusion bodies correlates with predicted aggregation rates. *J. Biotechnol. 125*, 110−113.

(8) de Groot, N. S., and Ventura, S. (2006) Effect of temperature on protein quality in bacterial inclusion bodies. *FEBS Lett. 580*, 6471−6476.

(9) Garcia-Fruitos, E., Gonzalez-Montalban, N., Morell, M., Vera, A., Ferraz, R. M., Aris, A., Ventura, S., and Villaverde, A. (2005) Aggregation as bacterial inclusion bodies does not imply inactivation of enzymes and fluorescent proteins. *Microb. Cell Fact 4*, 27.

(10) Martinez-Alonso, M., Vera, A., and Villaverde, A. (2007) Role of the chaperone DnaK in protein solubility and conformational quality in inclusion body-forming *Escherichia coli* cells. *FEMS Microbiol. Lett. 273*, 187−195.

(11) Martinez-Alonso, M., Garcia-Fruitos, E., and Villaverde, A. (2008) Yield, solubility and conformational quality of soluble proteins are not simultaneously favored in recombinant *Escherichia coli*. *Biotechnol. Bioeng. 101*, 1353−1358.

(12) Martinez-Alonso, M., Gonzalez-Montalban, N., Garcia-Fruitos, E., and Villaverde, A. (2008) The functional quality of soluble recombinant polypeptides produced in *Escherichia coli* is defined by a wide conformational spectrum. *Appl. Environ. Microbiol. 174*, 7431−7433.

(13) Garcia-Fruitos, E., Sabate, R., de Groot, N. S., Villaverde, A., and Ventura, S. (2011) Biological role of bacterial inclusion bodies: a model for amyloid aggregation. *FEBS J. 278*, 2419−2427.

(14) Vera, A., Gonzalez-Montalban, N., Aris, A., and Villaverde, A. (2007) The conformational quality of insoluble recombinant proteins is enhanced at low growth temperatures. *Biotechnol. Bioeng. 96*, 1101−1106.

(15) Peternel, S., Grdadolnik, J., Gaberc-Porekar, V., and Komel, R. (2008) Engineering inclusion bodies for non denaturing extraction of functional proteins. *Microbial Cell Factories 7*, 34.

(16) Tsumoto, K., Umetsu, M., Kumagai, I., Ejima, D., and Arakawa, T. (2003) Solubilization of active green fluorescent protein from insoluble particles by guanidine and arginine. *Biochem. Biophys. Res. Commun. 312*, 1383−1386.

(17) Rehm, B. H. A. (2006) Genetics and biochemistry of polyhydroxyalkanoate granule self-assembly: The key role of polyester synthases. *Biotechnol. Lett. 28*, 207−213.

(18) Grage, K., and Rehm, B. H. A. (2008) *In vivo* production of scFv-displaying biopolymer beads using a self-assembly-promoting fusion partner. *Bioconjugate Chem. 19*, 254−262.

(19) Jahns, A. C., Haverkamp, R. G., and Rehm, B. H. A. (2008) Multifunctional inorganic-binding beads self-assembled inside engineered bacteria. *Bioconjugate Chem. 19*, 2072−2080.

(20) Brockelbank, J. A., Peters, V., and Rehm, B. H. A. (2006) Recombinant *Escherichia coli* strain produces a ZZ domain displaying biopolyester granules suitable for immunoglobulin G purification. *Appl. Environ. Microbiol. 72*, 7394−7397.

(21) Grage, K., Jahns, A. C., Parlane, N., Palanisamy, R., Rasiah, I. A., Atwood, J. A., and Rehm, B. H. A. (2009) Bacterial polyhydroxyalkanoate granules: biogenesis, structure, and potential use as nano-/micro-beads in biotechnological and biomedical applications. *Biomacromolecules 10*, 660−669.

(22) Sambrook, J., Fritsch, E. F., and Maniatis, T. (1989) *Molecular cloning: a laboratory manual*, Cold Spring Harbor Laboratory Press, Plainview, NY.

(23) Amara, A. A., and Rehm, B. H. A. (2003) Replacement of the catalytic nucleophile cysteine-296 by serine in class II polyhydroxyalkanoate synthase from *Pseudomonas aeruginosa*-mediated synthesis of a new polyester: identification of catalytic residues. *Biochem. J. 374*, 413−421.

(24) Brandl, H., Gross, R. A., Lenz, R. W., and Fuller, R. C. (1988) *Pseudomonas oleovorans* as a source of poly(beta-hydroxyalkanoates) for potential applications as biodegradable polyesters. *Appl. Environ. Microbiol. 54*, 1977−1982.

(25) Laemmli, U. K. (1970) Cleavage of structural proteins during the assembly of the head of bacteriophage T4. *Nature 227*, 680−685.

(26) Bradford, M. M. (1976) A rapid and sensitive method for the quantitation of microgram quantities of protein utilizing the principle of protein-dye binding. *Anal. Biochem. 72*, 248−254.
(27) Peters, V., Becher, D., and Rehm, B. H. A. (2007) The inherent property of polyhydroxyalkanoate synthase to form spherical PHA granules at the cell poles: the core region is required for polar localization. *J. Biotechnol. 132*, 238−245.
(28) Mifune, J., Grage, K., and Rehm, B. H. A. (2009) Production of functionalized biopolyester granules by recombinant *Lactococcus lactis*. *Appl. Environ. Microbiol. 75*, 4668−4675.
(29) Rehm, B. H. A. (2010) Bacterial polymers: biosynthesis, modifications and applications. *Nat. Rev. Microbiol. 8*, 578−592.
(30) Rehm, B. H. A., Antonio, R. V., Spiekermann, P., Amara, A. A., and Steinbüchel, A. (2002) Molecular characterization of the poly(3-hydroxybutyrate) (PHB) synthase from *Ralstonia eutropha*: in vitro evolution, site-specific mutagenesis and development of a PHB synthase protein model. *Biochim. Biophys. Acta 1594*, 178−190.
(31) Ringenberg, M., Lichtensteiger, C., and Vimr, E. (2001) Redirection of sialic acid metabolism in genetically engineered Escherichia coli. *Glycobiology 11*, 533−539.
(32) Leffel, S. M., Mabon, S. A., and Stewart, C. N., Jr. (1997) Applications of green fluorescent protein in plants. *BioTechniques 23*, 912−918.
(33) Phillips, G. N., Jr. (1997) Structure and dynamics of green fluorescent protein. *Curr. Opin. Struct. Biol. 7*, 821−827.
(34) Naylor, L. H. (1999) Reporter gene technology: the future looks bright. *Biochem. Pharmacol. 58*, 749−757.
(35) Misteli, T., and Spector, D. L. (1997) Applications of the green fluorescent protein in cell biology and biotechnology. *Nat. Biotechnol. 15*, 961−964.
(36) Taylor, D. L., Woo, E. S., and Giuliano, K. A. (2001) Real-time molecular and cellular analysis: the new frontier of drug discovery. *Curr. Opin. Biotechnol. 12*, 75−81.
(37) Atwood, J. A., and Rehm, B. H. A. (2009) Protein engineering towards biotechnological production of bifunctional polyester beads. *Biotechnol. Lett. 31*, 131−137.
(38) Jahns, A. C., and Rehm, B. H. A. (2009) Tolerance of the *Ralstonia eutropha* class I polyhydroxyalkanoate synthase for translational fusions to its C terminus reveals a new mode of functional display. *Appl. Environ. Microbiol. 75*, 5461−5466.
(39) Peters, V., and Rehm, B. H. A. (2005) *In vivo* monitoring of PHA granule formation using GFP-labeled PHA synthases. *FEMS Microbiol. Lett. 248*, 93−100.
(40) Peternel, S., Gaberc-Porekar, V., and Komel, R. (2009) Bacterial growth conditions affect quality of GFP expressed inside inclusion bodies. *Acta Chim. Slov. 56*, 860−867.
(41) Vazquez, E., Cubarsi, R., Unzueta, U., Roldan, M., Domingo-Espin, J., Ferrer-Miralles, N., and Villaverde, A. (2010) Internalization and kinetics of nuclear migration of protein-only, arginine-rich nanoparticles. *Biomaterials 31*, 9333−9339.
(42) Rehm, B. H. A. (2003) Polyester synthases: natural catalysts for plastics. *Biochem. J. 376*, 15−33.
(43) Zhou, P., Lugovskoy, A. A., and Wagner, G. (2001) A solubility-enhancement tag (SET) for NMR studies of poorly behaving proteins. *J. Biomol. NMR 20*, 11−14.
(44) Inouye, S., and Sahara, Y. (2008) Soluble protein expression in *E. coli* cells using IgG-binding domain of protein A as solubilizing partner in the cold induced system. *Biochem. Biophys. Res. Commun. 376*, 448−453.
(45) Inouye, S., and Tsuji, F. I. (1994) Evidence for redox forms of the Aequorea green fluorescent protein. *FEBS Lett. 351*, 211−214.
(46) Ward, W. W., Prentice, H. J., Roth, A. F., Cody, C. W., and Reeves, S. C. (1982) Spectral Perturbations of the *Aequorea* green-fluorescent protein. *Photochem. Photobiol. 35*, 803−808.
(47) Fradkov, A. F., Verkhusha, V. V., Staroverov, D. B., Bulina, M. E., Yanushevich, Y. G., Martynov, V. I., Lukyanov, S., and Lukyanov, K. A. (2002) Far-red fluorescent tag for protein labelling. *Biochem. J. 368*, 17−21.